A note on analytic quadratic Brillouin zone integration

1993 J. Phys.: Condens. Matter 5 2321

(http://iopscience.iop.org/0953-8984/5/15/005)

J. Phys.: Condens. Matter 5 (1993) 2321–2332. Printed in the UK

A note on analytic quadratic Brillouin zone integration

R Winkler

Institut für Theoretische Physik, Universität Regensburg, D–8400 Regensburg, Germany

Received 23 November 1992, in final form 10 February 1993

Abstract. We propose an improved quadratic simplex method for evaluating surface and volume integrals in the Brillouin zone. The scheme that is commonly used for deriving a piecewise quadratic interpolation of the dispersion misweights the gridpoints with respect to their symmetry-induced multiplicity. We suggest subdividing the simplices into smaller ones for which different interpolating functions are obtained. In addition, we derive analytical expressions for both the surface and volume integral in two dimensions which properly take into account the integrable Van Hove singularities. As an example, we discuss the self-consistent calculation of the hole subband structure in a GaAs–AlGaAs heterojunction.

1. Introduction

In solid state physics we are frequently interested in surface and volume integrals of the form

$$I(E) = \int_{\mathcal{D}} f(\boldsymbol{k})\,\delta(E - \mathcal{E}(\boldsymbol{k}))\,\mathrm{d}^d\boldsymbol{k} = \int_{\mathcal{E}(\boldsymbol{k})=E} \frac{f(\boldsymbol{k})}{|\nabla\mathcal{E}(\boldsymbol{k})|}\,\mathrm{d}S(\boldsymbol{k}) \tag{1}$$

$$J(E) = \int_{\mathcal{D}} f(\boldsymbol{k})\,\theta(E - \mathcal{E}(\boldsymbol{k}))\,\mathrm{d}^d\boldsymbol{k}. \tag{2}$$

Here $\mathcal{E}(\boldsymbol{k})$ is the energy dispersion, $f(\boldsymbol{k})$ is a property function and the domain of integration $\mathcal{D}$ is the d-dimensional Brillouin zone (BZ). We have $I(E) = \frac{\mathrm{d}}{\mathrm{d}E}J(E)$. If $f(\boldsymbol{k}) \equiv 1$ then $I(E)$ is the density of states $D(E)$ (DOS). Other quantities that can be defined by such integrals are, for example, the charge density, conductivity, dielectric function and magnetic susceptibility [1–4].

Seldom are $\mathcal{E}$ and f given in terms of analytical expressions. Often we have to content ourselves with numerical values of $\mathcal{E}$ and f that are obtained on a coarse grid of $\boldsymbol{k}$-points from complicated time-consuming calculations such as total energy or self-consistent bandstructure calculations [5–7]. Hence the evaluation of I and J has to be based on an efficient interpolation of $\mathcal{E}$ and f.

Commonly $\mathcal{D}$ is restricted to an irreducible wedge of the Brillouin zone (IBZ). Inside the IBZ a piecewise linear interpolation is derived for $\mathcal{E}$ and f so that the integrals (1) and (2) can easily be evaluated analytically. This idea, which was originally introduced by Gilat and Raubenheimer [8], forms the basis of the most frequently used *linear simplex method* of Jepson and Anderson [9] and Lehmann and Taut [10]. These authors suggested replacing the integrals (1) and (2) by a sum of integrals over space-filling simplices Γ_ν. The subdivision is performed in such a way that the numerical values of $\mathcal{E}$ and f are known for the vertices of each simplex, thus defining the interpolating functions.

0953-8984/93/152321+12$07.50

Kleinman [11] has pointed out that, starting from a grid of k-points, different subdivisions of the IBZ can be found that will give different weights to the grid points in the linear interpolation scheme. But none of the subdivisions will weight the grid points according to their symmetry-induced multiplicity so that remarkable errors can occur (see also [12–14]). Kleinman suggested that for cubic crystals ($d = 3$) the domain of integration should be extended to a cubic super BZ consisting of two FCC BZ or four BCC BZ. His ansatz is equivalent to calculating $I(E)$ and $J(E)$ for different subdivisions of the IBZ such that on average the grid points are correctly weighted according to their symmetry-induced multiplicity. His approach was refined by Hama and co-workers [14], who showed that the computational effort can be greatly reduced when certain subdivisions are considered.

Van Hove proved in his famous theorem [15] that due to the periodicity of $\mathcal{E}(k)$ we always observe certain singularities in $D(E)$ for which $\nabla\mathcal{E}(k)$, i.e. the denominator in (1), vanishes. These singularities become more pronounced for lower d. In order to treat them properly we have to use an interpolation of $\mathcal{E}$ that is (at least) quadratic in k. Thus to improve convergence of the linear simplex method, MacDonald and co-workers [16] suggested the *hybrid simplex method*. Starting from the coarser grid of k-points a quadratic interpolation for $\mathcal{E}(k)$ is derived. It is used to define a finer grid of k-points, which can be evaluated by applying the standard linear simplex method.

Recently Boon, Methfessel and Mueller (BMM) [17–19] and Wiesenekker, Velde and Baerends (WVB) [20, 21] succeeded in evaluating $I(E)$ analytically for a piecewise quadratic interpolation of $\mathcal{E}$ in $d = 2$ and 3 dimensions *(quadratic simplex method)* so that their methods converge much faster than the linear simplex method.

In order to obtain a piecewise quadratic interpolation for $\mathcal{E}$ and f they suggested subdividing the IBZ into space-filling simplices Γ_ν such that the numerical values of $\mathcal{E}$ and f are given at the vertices and midpoints of the edges. This choice appears to be natural because the $(d+1)(d+2)/2$ expansion coefficients needed for a quadratic interpolation can be fixed uniquely in that way. In addition the interpolation is continuous at the interfaces of Γ_ν. They did not take into consideration that this ansatz misweights the grid points in a manner similar to the linear simplex method.

The integration schemes of both BMM and WVB are analytic in nature. BMM restricted the expansion of $f(k)$ to first order in k. Thus they were able to obtain an expression for $I(E)$ which, as we will show, can be integrated analytically to get $J(E)$. WVB used an algebraic approach based on an expansion of both $\mathcal{E}(k)$ and $f(k)$ up to second order in k. This makes it more accurate when evaluating $I(E)$. But as they could not find an analytical expression for $J(E)$, they suggested a numerical integration scheme for deriving J from I. While the computational effort of BMM compares well with the linear simplex method, it is considerably larger for the second approach.

In this paper we suggest some improvements on quadratic BZ integration in order to overcome its shortcomings noted above. First, we propose a piecewise quadratic interpolatory scheme that properly weights the grid points with respect to their symmetry induced multiplicity. Second, based on BMM, we derive analytical expressions for both $I(E)$ and $J(E)$ in $d = 2$ dimensions. In that way we properly treat the integrable Van Hove singularities in $I(E)$ when $J(E)$ is calculated.

As an application to semiconductor physics we present in section 4 results of a self-consistent calculation of the DOS effective mass of holes in a GaAs–$Al_{0.5}Ga_{0.5}As$ heterostructure. The corresponding hole subbands are known to have a rather anisotropic and non-parabolic dispersion $\mathcal{E}(k)$ [22].

2. Interpolation of $\mathcal{E}$ and f

In the linear simplex method the BZ is divided into space-filling simplices Γ_ν such that the numerical values of $\mathcal{E}$ and f in the $d+1$ vertices of each simplex provide a linear interpolation that can be evaluated analytically. Two examples of a subdivision for $d = 2$ are shown in figure 1.

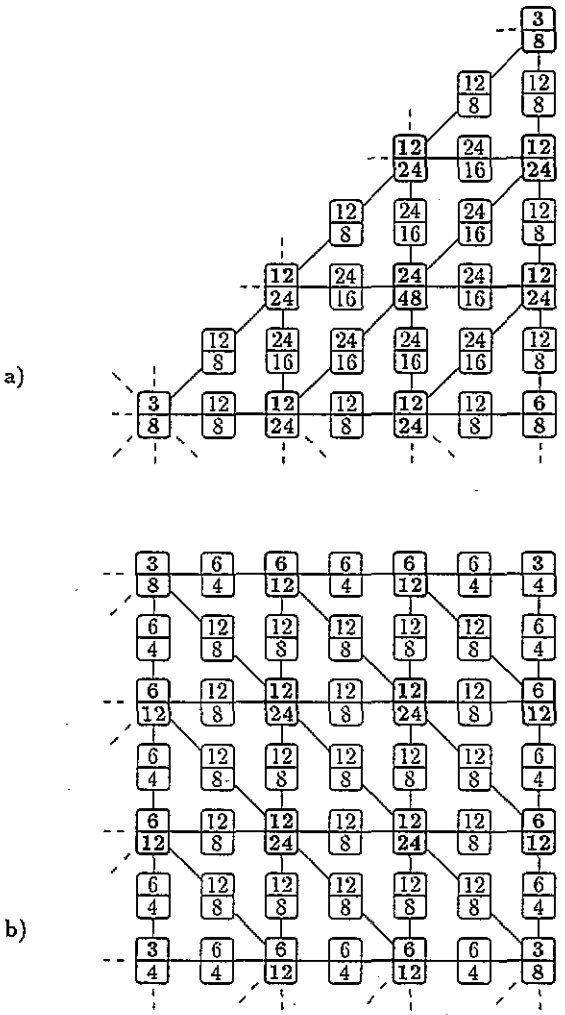

Figure 1. (*a*) Subdivision into triangles of the irreducible wedge of the two-dimensional quadratic BZ. The grid points are denoted $\begin{smallmatrix}\mathbf{i}\\ \mathbf{j}\end{smallmatrix}$; i is its weight according to its symmetry-induced multiplicity, and j its weight in the quadratic interpolatory scheme (both in multiples of 1/432, so that their sum equals 1). Those printed in bold correspond to vertices of the triangles shown, hence they are relevant for a linear interpolatory scheme. For a quadratic interpolation we also need the other grid points at the midpoints of the edges. (*b*) Another subdivision of the BZ with proper symmetry.

The basic idea of the quadratic simplex method is similar. The interpolation of $\mathcal{E}(\boldsymbol{k})$ is based on a second-order expansion

$$\mathcal{E}(\boldsymbol{k}) = \mathcal{E}^{(0)} + \mathcal{E}^{(1)}\boldsymbol{k} + \boldsymbol{k}\,\mathcal{E}^{(2)}\boldsymbol{k} \tag{3}$$

where $\mathcal{E}^{(1)}$ is a d-dimensional vector and $\mathcal{E}^{(2)}$ is a symmetric $d \times d$ matrix. A similar expression holds for $f(\boldsymbol{k})$. We require $(d+1)(d+2)/2$ numerical values of $\mathcal{E}$ and f in order to fix the expansion coefficients in (3). Commonly the subdivision is chosen such that $\mathcal{E}$ and f are given for the vertices and midpoints of the edges of the simplices Γ_ν, see figure 1.

At first glance it seems reasonable to restrict the procedure outlined above to an IBZ. But as pointed out by Kleinman [11], it is impossible to find a subdivision of the IBZ into simplices which correctly weights the grid points according to their symmetry-induced multiplicity. This can result in remarkable errors in $I(E)$ and $J(E)$. In figure 1 we illustrate this point for two subdivisions of a two-dimensional BZ. We compare the weight of the grid points due to its symmetry-induced multiplicity with the weights that are assigned to these points in a quadratic interpolatory scheme.

Kleinman [11] and Hama, Watanabe and Koto [14] argued that we have to extend the domain of integration to some larger part of $\boldsymbol{k}$ space such that we average over the values of $I(E)$ and $J(E)$ obtained for different subdivisions. When generalizing their idea to the quadratic simplex method we have to consider subdivisions (in addition to those in figure 1) where the role of grid points as being placed at the vertices and midpoints of the edges is interchanged. For example, one finds eight non-equivalent subdivisions of the two-dimensional BZ that must be taken into consideration in a quadratic integration scheme.

We suggest a slightly different approach, which might make it more obvious that the reason for these difficulties is that an inappropriate interpolation of $\mathcal{E}$ and f is used. This means that we can either average on the final results $I(E)$ and $J(E)$ obtained for different interpolating functions $\mathcal{E}(\boldsymbol{k})$ and $f(\boldsymbol{k})$ (as in [11, 14]), or we can derive from the beginning proper interpolating functions $\mathcal{E}(\boldsymbol{k})$ and $f(\boldsymbol{k})$ that will satisfy crystal symmetry and correctly weight the grid points so that it becomes possible to restrict the domain of integration to an IBZ.

We note that if we derive the interpolating functions $\mathcal{E}(\boldsymbol{k})$ and $f(\boldsymbol{k})$ in the usual way described above, these functions are not unique. Let us consider a point $\boldsymbol{k}_0$ somewhere in the BZ. The values $\mathcal{E}(\boldsymbol{k}_0)$ and $f(\boldsymbol{k}_0)$ sensitively depend on which of the surrounding grid points are taken into account when we determine the expansion coefficients in (3). To be more specific we again consider a quadratic interpolation in the two-dimensional BZ. For each of the small triangles Δ_μ (see figure 2) we find eight basic triangles Γ that might be used to fix the six expansion coefficients in (3). These eight sets of expansion coefficients have to be averaged in order to obtain a proper interpolation of $\mathcal{E}$ and f within Δ_μ. Hence we subdivide the IBZ into triangles Δ_μ, which are evaluated separately. We remark that the quadratic interpolation is continuous at the edges of Δ_μ.

Our ansatz can be readily generalized to higher dimensions d and arbitrary orders of expansion of $\mathcal{E}(\boldsymbol{k})$ and $f(\boldsymbol{k})$, but it seems to have no computational advantage over the approach of Kleinman. In both cases we have to sum (for $d = 2$) over eight times as many simplices compared with a simple subdivision shown in figure 1(a). However the advantage of our procedure will become clear in subsection 3.4.

In practical calculations we have to bear in mind that at $\boldsymbol{k}$-points of high symmetry it is possible that two bands can touch each other. But at neighbouring points in $\boldsymbol{k}$-space this degeneracy is lifted and the bands repel each other (we assume that bands are labelled in order of increasing energy; see also figure 2 in [23]). Gilat [24] pointed out that in these cases interpolatory schemes may lead to 'fortuitous' singularities in the DOS, which are particularly pronounced if quadratic instead of linear interpolation is used. Obviously we

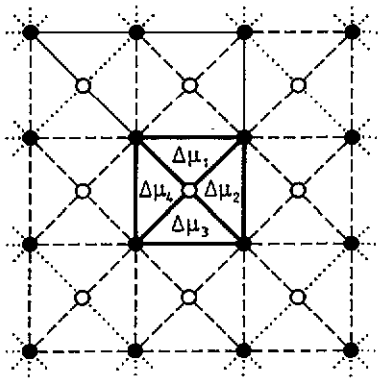

Figure 2. Full circles • represent some part of a regular grid of k-points ($d = 2$). For each of the small triangles Δ_μ (bold lines) we find eight larger triangles Γ (broken lines) which might provide a quadratic interpolation within Δ_μ. One such triangle Γ is marked with thin full lines; it might give an interpolation within Δ_{μ_1} and Δ_{μ_2}. Open circles ○ represent additional grid points that are used in the hybrid method.

can avoid these difficulties if the degeneracy occurs at an apex of the IBZ so that this point can be used as a grid point of our calculation. This is the case in the example discussed in section 4. But in general these points can lie anywhere along an axis of high symmetry. In simplices Δ_μ containing such points the dispersion $\mathcal{E}(\boldsymbol{k})$ will not be exactly reproduced by a single interpolating function of first or second order in $\boldsymbol{k}$. Nevertheless we want to emphasize that *properly* chosen interpolating functions $\mathcal{E}(\boldsymbol{k})$ of second order in $\boldsymbol{k}$ yield more accurate results than a linear interpolation. The reason for this is that each of these functions is used in a simplex Δ_μ which is actually smaller than the simplices Γ_ν that are normally used for a piecewise linear interpolation (see figure 2).

3. Evaluation of $I(E)$ and $J(E)$

After having established proper second-order expansions $\mathcal{E}(\boldsymbol{k})$ and $f(\boldsymbol{k})$ we consider the evaluation of the integrals $I(E)$ and $J(E)$ within Δ_μ for $d = 2$. Three cases will be distinguished: (i) $\mathcal{E}(\boldsymbol{k}) = \mathcal{E}^{(0)}$, $\det \mathcal{E}^{(2)} = |\mathcal{E}^{(1)}| = 0$; (ii) $\mathcal{E}(\boldsymbol{k}) = \mathcal{E}^{(0)} + \mathcal{E}^{(1)}\boldsymbol{k}$, $\det \mathcal{E}^{(2)} = 0$; (iii) $\mathcal{E}(\boldsymbol{k}) = \mathcal{E}^{(0)} + \mathcal{E}^{(1)}\boldsymbol{k} + \boldsymbol{k}\mathcal{E}^{(2)}\boldsymbol{k}$, $\det \mathcal{E}^{(2)} \neq 0$. The rarely occurring case of a singular yet non-vanishing matrix $\mathcal{E}^{(2)}$ can be included in (ii) by means of the hybrid method (subsection 3.4). We believe that the more elaborate discussion by WVB is in general not necessary. In the forthcoming we neglect for brevity the sum over Δ_μ.

3.1. The constant case

A constant energy dispersion gives the simple relation

$$I(E) = \delta(E - \mathcal{E}^{(0)}) \int_\Delta f(\boldsymbol{k})\, \mathrm{d}^2\boldsymbol{k}. \tag{4}$$

Now the $\boldsymbol{k}$ integral only depends on f and even a quadratic expansion of that function can be used. One obtains [20]

$$\int_\Delta f(\boldsymbol{k})\, \mathrm{d}^2\boldsymbol{k} = \tfrac{1}{3} V\, (f_{12} + f_{23} + f_{31}) \tag{5}$$

where f_{ij} are the values of f at the midpoints of the triangle edges and V is the area of Δ. Obviously if $J(E)$ has to be evaluated for $E > \max_{k\in\Delta}\{\mathcal{E}(k)\}$ then (5) is also applicable when $\mathcal{E}(k)$ is not constant.

3.2. The linear case

The well known formulae for the linear tetrahedron method ($d = 3$) can be generalized to arbitrary dimensions d [25]. We find for $d = 2$

$$J(E) = 0 \qquad E < \mathcal{E}_1 \tag{6a}$$

$$J(E) = \frac{(E-\mathcal{E}_1)^2}{(\mathcal{E}_2-\mathcal{E}_1)(\mathcal{E}_3-\mathcal{E}_1)}\left[f_1 + \tfrac{1}{3}(E-\mathcal{E}_1)\left(\frac{f_2-f_1}{\mathcal{E}_2-\mathcal{E}_1}+\frac{f_3-f_1}{\mathcal{E}_3-\mathcal{E}_1}\right)\right] \qquad \mathcal{E}_1 < E < \mathcal{E}_2 \tag{6b}$$

$$J(E) = V\left\{\tfrac{1}{3}(f_1+f_2+f_3) - \frac{(E-\mathcal{E}_3)^2}{(\mathcal{E}_1-\mathcal{E}_3)(\mathcal{E}_2-\mathcal{E}_3)} \times\left[f_3 + \tfrac{1}{3}(E-\mathcal{E}_3)\left(\frac{f_1-f_3}{\mathcal{E}_1-\mathcal{E}_3}+\frac{f_2-f_3}{\mathcal{E}_2-\mathcal{E}_3}\right)\right]\right\} \qquad \mathcal{E}_2 < E < \mathcal{E}_3 \tag{6c}$$

$$J(E) = \tfrac{1}{3}V(f_1+f_2+f_3) \qquad \mathcal{E}_3 < E \tag{6d}$$

$$I(E) = \frac{\mathrm{d}}{\mathrm{d}E}J(E) \tag{7}$$

where $\mathcal{E}_i$ and f_i are the values of $\mathcal{E}$ and f at the ith vertex of Δ. It is assumed that the tuples $(\mathcal{E}_i, f_i)$ are ordered according to $\mathcal{E}_1 \leqslant \mathcal{E}_2 \leqslant \mathcal{E}_3$. Note the difference between (5) and (6d).

3.3. The quadratic case

We give a discussion of the quadratic case, which is improved in some points compared to BMM in [18, 19]. We start with $f(k) \equiv 1$, looking for an analytic expression for $D(E)$. If both eigenvalues of $\mathcal{E}^{(2)}$ have the same sign, the surface of constant energy $S(E)$ is an ellipse, otherwise it is a hyperbola. This suggests we should change over to new coordinates that give a better parametrization of $S(E)$ than cartesian coordinates. To do this we first shift the coordinate and energy scale so that both $\mathcal{E}^{(0)}$ and $\mathcal{E}^{(1)}$ vanish. For brevity we will use the same notation for the shifted dispersion $\mathcal{E}(k) = k\mathcal{E}^{(2)}k$.

Next, we can make a transformation to principal axes and change the scale so that $\mathcal{E}(k') = \pm k_x'^2 \pm k_y'^2$, although in general it is not necessary to do that explicitly. We obtain

$$D(E) = \frac{1}{\sqrt{|\det \mathcal{E}^{(2)}|}}\int_\Delta \delta(E \mp k_x'^2 \mp k_y'^2)\mathrm{d}^2k'. \tag{8}$$

If both eigenvalues of $\mathcal{E}^{(2)}$ have the same sign, we use modified polar coordinates $k_x' = \sqrt{\varepsilon}\cos\varphi$ and $k_y' = \sqrt{\varepsilon}\sin\varphi$, leading to

$$D(E) = \frac{1}{2\sqrt{|\det \mathcal{E}^{(2)}|}}\int \delta(E-\varepsilon)\mathrm{d}\varepsilon \int \mathrm{d}\varphi. \tag{9}$$

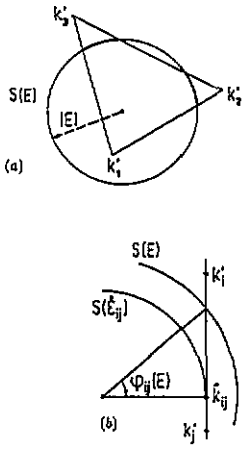

Figure 3. (*a*) The density of states is proportional to the angle of the bold marked part of a surface of constant energy $S(E)$ which lies inside the triangle. (*b*) The surface of constant energy $S(\hat{\mathcal{E}}_{ij})$ touches the line $k_i'k_j'$ tangentially at $\hat{k}_{ij}$. $\varphi_{ij}(E)$ is half the angle that $k_i'k_j'$ cuts out of $S(E)$.

Hence $D(E)$ is proportional to the angle φ of $S(E)$ which lies inside Δ; it corresponds to the bold marked part of $S(E)$ shown in figure 3(*a*).

The vertices of Δ are denoted by $\boldsymbol{k}_i$ and $\mathcal{E}_i \equiv \mathcal{E}(\boldsymbol{k}_i)$. Associated with the edge $[\boldsymbol{k}_i, \boldsymbol{k}_j]$ there is an energy $\hat{\mathcal{E}}_{ij}$ such that $S(\hat{\mathcal{E}}_{ij})$ touches the line $\boldsymbol{k}_i\boldsymbol{k}_j$ tangentially at a point $\hat{\boldsymbol{k}}_{ij}$, see figure 3(*b*). The energy $\hat{\mathcal{E}}_{ij}$ is related to the angle $\varphi_{ij}(E)$ by

$$\varphi_{ij}(E) = \cos^{-1}(\sqrt{\hat{\mathcal{E}}_{ij}/E}) \tag{10}$$

where φ_{ij} is half the angle that the line $\boldsymbol{k}_i\boldsymbol{k}_j$ will cut out of $S(E)$. Note that $\varphi_{ij}(E)$ only depends on $\hat{\mathcal{E}}_{ij}$, which is invariant under the transformation $\boldsymbol{k} \to \boldsymbol{k}'$.

The angle $\varphi_{ij}(E)$ describes how $D(E)$ changes when E sweeps over the interval defined by $\mathcal{E}_i$, $\mathcal{E}_j$ and $\hat{\mathcal{E}}_{ij}$. Hence to get $D(E)$ we sum $\varphi_{ij}(E)$ over the three edges of Δ with an appropriate sign σ_{ij}, weight $w_{ij}(E)$ and constant of integration $c(E)$:

$$D(E) = \frac{1}{2\sqrt{|\det \mathcal{E}^{(2)}|}} \sum \sigma_{ij}\, w_{ij}(E)\, \varphi_{ij}(E) + c(E). \tag{11}$$

(i) The sign σ_{ij} is '$-$' ('$+$') if the origin of the coordinate frame lies on the same (opposite) side of the line $\boldsymbol{k}_i\boldsymbol{k}_j$ as the third vertex of the triangle.

(ii) We have $w_{ij}(E) = 2$ if $S(\hat{\mathcal{E}}_{ij})$ touches the line $\boldsymbol{k}_i\boldsymbol{k}_j$ inside the edge $[\boldsymbol{k}_i, \boldsymbol{k}_j]$ and E lies inside the interval defined by $\hat{\mathcal{E}}_{ij}$ and the closer of the apex energies $\mathcal{E}_i$, $\mathcal{E}_j$.

(iii) We have $w_{ij}(E) = 1$ if E lies inside the interval $[\mathcal{E}_i, \mathcal{E}_j]$.

(iv) Otherwise we have $w(E) = 0$.

(v) In order to determine the constants of integration within the intervals defined by $\mathcal{E}_i$ and $\hat{\mathcal{E}}_{ij}$ we take advantage of the continuity of $D(E)$: $c(E)$ becomes a step function that is chosen such that it removes discontinuities introduced by $w_{ij}(E)$ at $\mathcal{E}_i$ and $\hat{\mathcal{E}}_{ij}$, except for a jump of 2π at $E = 0$ if the origin of the coordinate frame lies inside the triangle.

The integral of (11) is $N(E) \equiv \int^E D(E')\,\mathrm{d}E'$. Starting from

$$\Phi_{ij}(E) \equiv \int^E \varphi_{ij}(E')\,\mathrm{d}E' = E\cos^{-1}(\sqrt{\hat{\mathcal{E}}_{ij}/E}) - \hat{\mathcal{E}}_{ij}\sqrt{(E/\hat{\mathcal{E}}_{ij}) - 1} \tag{12}$$

we obtain $N(E)$ in a way similar to $D(E)$.

If the eigenvalues of $\mathcal{E}^{(2)}$ are opposite in sign we use modified hyperbolic coordinates. We obtain

$$\varphi_{ij}(E) = -\ln\bigl(\sqrt{|\hat{\mathcal{E}}_{ij}/E|} + \sqrt{|(\hat{\mathcal{E}}_{ij}/E) - 1|}\bigr). \tag{13}$$

When we applied the analytic quadratic integration scheme to the simple tight-binding band $\mathcal{E}(\boldsymbol{k}) = -\frac{1}{2}(\cos\pi k_x + \cos\pi k_y)$, as suggested by BMM, we found it necessary to treat one special case separately. It might happen that an edge $[\boldsymbol{k}'_i, \boldsymbol{k}'_j]$ of the triangle is almost parallel to the light cone defined by the Minkowski metric $\mathcal{E}(\boldsymbol{k}') = \pm(k'^2_x - k'^2_y)$. Hence $\hat{\boldsymbol{k}}_{ij}$ and $\hat{\mathcal{E}}_{ij}$ are ill defined. In that case we suggest performing the affine transformation $\boldsymbol{k} \to \boldsymbol{k}'$ explicitly. Now we can determine the hyperbolic angle of a point on the edge $[\boldsymbol{k}'_i, \boldsymbol{k}'_j]$ from its energy E and the cartesian coordinates of the vertices $\boldsymbol{k}'_i$ and $\boldsymbol{k}'_j$. We find

$$\varphi_{ij}(E) = \tfrac{1}{2}\ln|\alpha + \beta E| \tag{14}$$

where

$$\begin{aligned}
\alpha &= (1/\gamma)[k'_{iy}\mathcal{E}_j - k'_{jy}\mathcal{E}_i + \sigma(k'_{ix}\mathcal{E}_j - k'_{jx}\mathcal{E}_i)] \\
\beta &= (2/\gamma)[k'_{jy} - k'_{iy}] \\
\gamma &= k'_{iy}\mathcal{E}_j - k'_{jy}\mathcal{E}_i - \sigma(k'_{ix}\mathcal{E}_j - k'_{jx}\mathcal{E}_i) \\
\sigma &= \operatorname{sgn}[(k'_{jx} - k'_{ix})(k'_{jy} - k'_{iy})].
\end{aligned}$$

BMM have shown that the above formulae can be generalized to deal with a linear function $f(\boldsymbol{k}) = f^{(0)} + \boldsymbol{f}^{(1)}\boldsymbol{k}$. The contribution of the second term can be evaluated with Gauss's theorem:

$$\begin{aligned}
\int_\Delta \boldsymbol{f}^{(1)}\boldsymbol{k}\delta(E - \boldsymbol{k}\mathcal{E}^{(2)}\boldsymbol{k})\mathrm{d}^2\boldsymbol{k} &= -\tfrac{1}{2}\int_\Delta \nabla\bigl[\boldsymbol{f}^{(1)}[\mathcal{E}^{(2)}]^{-1}\theta(E - \boldsymbol{k}\mathcal{E}^{(2)}\boldsymbol{k})\bigr]\mathrm{d}^2\boldsymbol{k} \\
&= -\tfrac{1}{2}\int_{\partial\Delta} \boldsymbol{f}^{(1)}[\mathcal{E}^{(2)}]^{-1}\boldsymbol{n}\theta(E - \boldsymbol{k}\mathcal{E}^{(2)}\boldsymbol{k})\mathrm{d}S(\boldsymbol{k}) \\
&= -\tfrac{1}{2}\boldsymbol{f}^{(1)}[\mathcal{E}^{(2)}]^{-1}\sum_{i=1}^{3}\boldsymbol{n}_i\int_{(\partial\Delta)_i}\theta\left(E - \boldsymbol{k}\mathcal{E}^{(2)}\boldsymbol{k}\right)\mathrm{d}\boldsymbol{k}
\end{aligned} \tag{15}$$

where $\boldsymbol{n}_i$ are unit vectors normal to the edges of the triangle. Hence for calculating $I(E)$ we need the one-dimensional integrated DOS $N^1_{ij}(E) \equiv \int^E D^1_{ij}(E')\,\mathrm{d}E'$ along the edges $[\boldsymbol{k}_i, \boldsymbol{k}_j]$. The corresponding one-dimensional dispersion $\mathcal{E}^1(\boldsymbol{k})$ can be readily derived from its two-dimensional counterpart. In general $\mathcal{E}^1(\boldsymbol{k})$ will be quadratic, except for a linear dispersion, which occurs when the edge is parallel to the light cone. Finally $J(E)$ is obtained in a similar way from $\Phi_{ij}(E)$ and the integrals of $N^1_{ij}(E)$. All formulae are summarized in table 1. We want to mention that the integrals needed for $J(E)$ always remain finite, even in the case of a Van Hove singularity in $I(E)$.

Table 1. Important formulae in the analytic quadratic BZ integration. We have that $a \equiv [(k_l - k_j)\mathcal{E}^{(2)}(k_l - k_j)]/\|k_l - k_j\|^2$ and $b \equiv |\mathcal{E}_l - \mathcal{E}_j|/\|k_l - k_j\|$.

Constant energy surface	Ellipse	Hyperbola	Light cone
Normal form	$\pm(k_x'^2 + k_y'^2)$	$\pm(k_x'^2 - k_y'^2)$	$\pm(k_x'^2 - k_y'^2)$
$\varphi_{ij}(E)$	$\cos^{-1}\left(\sqrt{\hat{\mathcal{E}}_{ij}/E}\right)$	$-\ln\left(\sqrt{\lvert\hat{\mathcal{E}}_{ij}/E\rvert} + \sqrt{\lvert\hat{\mathcal{E}}_{ij}/E - 1\rvert}\right)$	$\frac{1}{2}\ln\lvert\alpha + \beta E\rvert$
$\Phi_{ij}(E)$	$E\cos^{-1}\left(\sqrt{\hat{\mathcal{E}}_{ij}/E}\right) - \hat{\mathcal{E}}_{ij}\sqrt{E/\hat{\mathcal{E}}_{ij} - 1}$	$-E\ln\left(\sqrt{\lvert\hat{\mathcal{E}}_{ij}/E\rvert} + \sqrt{\lvert\hat{\mathcal{E}}_{ij}/E - 1\rvert}\right) + \hat{\mathcal{E}}_{ij}\sqrt{1 - E/\hat{\mathcal{E}}_{ij}}$	$\frac{1}{2}[(E + \alpha/\beta)\ln\lvert\alpha + \beta E\rvert - E]$
Edge: $N_{ij}^1(E)$	$2\mathrm{sgn}\,(a)\sqrt{E/a}$	$2\mathrm{sgn}\,(a)\sqrt{E/a}$	$E/\lvert b\rvert$
$\int^E N_{ij}^1(E')\,\mathrm{d}E'$	$\frac{4}{3}\lvert E\rvert^{3/2}/\lvert a\rvert^{1/2}$	$\frac{4}{3}\lvert E\rvert^{3/2}/\lvert a\rvert^{1/2}$	$\frac{1}{2}E^2/\lvert b\rvert$

3.4. The hybrid method

BMM suggested a least-squares fit to obtain a linear (first-order) expansion for $f(\boldsymbol{k})$ within each triangle. This yields an interpolation of $f(\boldsymbol{k})$ that is discontinuous at the edges of the triangles, so that artificial singularities are introduced in $I(E)$ and $J(E)$. Nevertheless, while a quadratic (second-order) expansion of $\mathcal{E}(\boldsymbol{k})$ is essential to account for Van Hove singularities in the DOS, there is no fundamental need to use a quadratic expansion of $f(\boldsymbol{k})$.

Due to the subdivision into smaller triangles Δ_μ discussed in section 2, we are led to a hybrid method [16] for $f(\boldsymbol{k})$ in a natural way (except for the cases where (5) is applicable). The second-order interpolation for $f(\boldsymbol{k})$ provides proper values for the 'additional' grid points (open circles in figure 2). They are used to derive a linear interpolation of f within each triangle Δ_μ so that (15) becomes applicable. This concept allows us to deal with strongly varying functions $f(\boldsymbol{k})$. Its convergence compares well with WVB, but it keeps the advantage of BMM that we can integrate analytically over Van Hove singularities when calculating $J(E)$.

4. Example

In layered semiconductor structures like inversion layers and quantum wells a quasi-two-dimensional electron or hole gas can be realized. The interfaces behave like a confining potential while the in-plane motion remains continuous. Therefore the electron- and hole-like states are characterized by a discrete quantum number i for the quantization in the growth direction and a two-dimensional wavevector $\boldsymbol{k} = (k_x, k_y)$ for the in-plane motion. The evaluation of two-dimensional $\boldsymbol{k}$-space integrals is an important step within the self-consistent calculation of these states.

As an example we discuss the hole subband structure in a GaAs–$Al_{0.5}Ga_{0.5}As$ heterojunction. We assume a hole concentration $N_s = 5 \times 10^{11}\,\mathrm{cm}^{-2}$, and the concentration of space charges in the GaAs depletion layer is $N_d = 1 \times 10^{13}\,\mathrm{cm}^{-3}$. This system has been investigated experimentally [26] as well as theoretically [22].

Our description is based on the 4×4 Luttinger Hamiltonian. We use a quadrature method for the coupled integral equations in momentum space to calculate the multicomponent spin-split envelope function $\xi_{i\sigma}(\boldsymbol{k}, z)$†. The Hartree potential is determined self-consistently from the charge density

$$\rho(z) = \frac{1}{4\pi^2} \sum_{i\sigma} \int \theta[\mathcal{E}_{i\sigma}(\boldsymbol{k}) - \mathcal{E}_F]\, |\xi_{i\sigma}(\boldsymbol{k}, z)|^2 \, \mathrm{d}^2k. \tag{16}$$

Note that the energy scale for holes is reversed, i.e. $\rho(z)$ results from occupied states above $\mathcal{E}_F$. The anisotropic and spin-split subband dispersion $\mathcal{E}_{i\sigma}(\boldsymbol{k})$ is shown in figure 4. It is used to calculate the DOS effective mass

$$\frac{m^*_{i\sigma}(E)}{m_0} = \frac{1}{\pi} \frac{\hbar^2}{2m_0} \int \delta(\mathcal{E}_{i\sigma}(\boldsymbol{k}) - E)\, \mathrm{d}^2k \tag{17}$$

which is presented in figure 5. One can easily trace back the singularities of $m^*_{i\sigma}(E)$ to the extrema of $\mathcal{E}_{i\sigma}(\boldsymbol{k})$. In figure 5 we compare the exact converged results obtained for a rather fine grid of $\boldsymbol{k}$-points with those for a coarser grid. The numerical results for the latter case agree much better with the former, if correctly weighted $\boldsymbol{k}$-points are used. We think that in many applications the increased computational effort of a proper interpolation is justified by the increase in accuracy that can be achieved, in particular when BZ integration is only a small part of much larger computations.

† The details of these calculations will be published elsewhere.

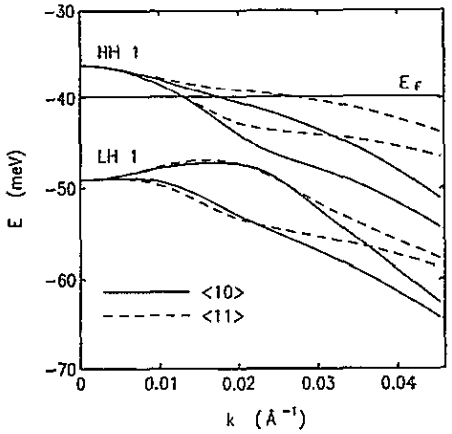

Figure 4. Anisotropic and spin split hole subband dispersion $\mathcal{E}_{i\sigma}(\boldsymbol{k})$ in a GaAs–$Al_{0.5}Ga_{0.5}As$ heterojunction for $N_s = 5 \times 10^{11}\,cm^{-2}$ and $N_d = 1 \times 10^{13}\,cm^{-3}$. The full curves correspond to $\boldsymbol{k}$ in ⟨10⟩ direction, while the broken curves are for ⟨11⟩.

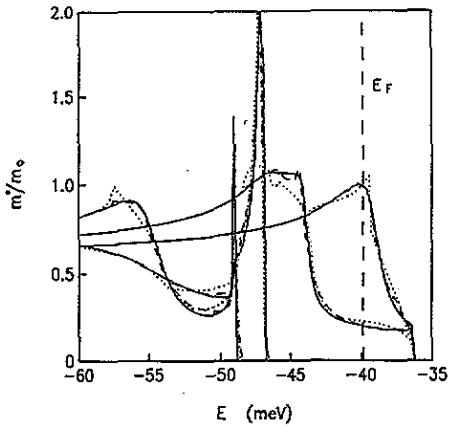

Figure 5. Calculated DOS effective mass $m^*_{i\sigma}(E)$ corresponding to the subband dispersion shown in figure 4. The full curves are based on a grid of $\boldsymbol{k}$-points with $\Delta k_x = \Delta k_y = 0.002\,Å^{-1}$, for the broken and dotted curves we used $\Delta k_x = \Delta k_y = 0.008\,Å^{-1}$. For the dotted line the interpolating quadratic form (3) was derived from only one subdivision similar to figure 1(*a*), hence one can see the insufficiencies of incorrectly weighted grid points.

5. Summary and conclusions

First, we have pointed out that for evaluating surface and volume integrals in the d-dimensional BZ we need a properly chosen interpolation of both $\mathcal{E}(\boldsymbol{k})$ and $f(\boldsymbol{k})$ in order to weight the grid points according to their symmetry-induced multiplicity. We find that the simplices have to be divided into smaller ones for which different interpolating functions must be used. Second, we have suggested some improvements on the quadratic BZ integration method of BMM to overcome its shortcomings compared with WVB while keeping its advantage that both the surface integral $I(E)$ and the volume integral $J(E)$ can be calculated analytically. Hence, Van Hove singularities are properly taken into account. The analytical evaluation of $J(E)$ is in particular useful when this quantity is needed only for a few values of E, e.g. at the Fermi energy $\mathcal{E}_F$, and $I(E)$ is not needed at all. Such an example was given in (16).

As an example we have applied the two-dimensional quadratic BZ integration method in the self-consistent calculation of the hole subband structure in a GaAs–AlGaAs heterojunction.

It is noteworthy that, compared with previous work, in our approach subdividing the domain of integration into space-filling simplices has become less important. In some cases it might be preferable that the quadratic form (3) is derived by means other than averaging over a certain class of simplices. Moreover our discussion in section 3.3 on the evaluation of the quadratic form can be readily generalized to arbitrary convex polygons.

Acknowledgments

The author wishes to thank F Bolton and U Rössler for critically reading the manuscript. Financial support by the Deutsche Forschungsgemeinschaft is gratefully acknowledged.

References

[1] Charlier J C, Gonze X and Michenaud J P 1991 *Phys. Rev.* B **43** 4579
[2] Ching W Y, Yong-Nian Xu and Wong K W 1989 *Phys. Rev.* B **40** 7684
[3] Alouani M, Brey L and Christensen N E 1988 *Phys. Rev.* B **37** 1167
[4] Callaway J, Chatterjee A K, Singhal S P and Ziegler A 1983 *Phys. Rev.* B **28** 3818
[5] Yong-Nian Xu and Ching W Y 1991 *Phys. Rev.* B **43** 4461
[6] Sigalas M, Bacalis N C, Papaconstantopoulos D A, Mehl M J and Switendick A C 1990 *Phys. Rev.* B **42** 11637
[7] Zandiehnadem F and Ching W Y 1990 *Phys. Rev.* B **41** 12162
[8] Gilat G and Raubenheimer L J 1966 *Phys. Rev.* **144** 390
[9] Jepson O and Anderson O K 1971 *Solid State Commun.* **9** 1763
[10] Lehmann G and Taut M 1972 *Phys. Status Solidi (b)* **54** 469
[11] Kleinman L 1983 *Phys. Rev.* B **28** 1139
[12] Jepsen O and Andersen O K 1984 *Phys. Rev.* B **29** 5965
[13] Hanke M, Kühn W and Strehlow R 1984 *Phys. Status Solidi (b)* **123** K39
[14] Hama J, Watanabe M and Kato T 1990 *J. Phys.: Condens. Matter* **2** 7445
[15] Van Hove L 1953 *Phys. Rev.* **89** 1189
[16] MacDonald A H, Vosko S H and Coleridge P T 1979 *J. Phys. C: Solid State Phys.* **12** 2991
[17] Methfessel M S, Boon M H and Mueller F M 1983 *J. Phys. C: Solid State Phys.* **16** L949
[18] Boon M H, Methfessel M S and Mueller F M 1986 *J. Phys. C: Solid State Phys.* **19** 5337
[19] Methfessel M S, Boon M H and Mueller F M 1987 *J. Phys. C: Solid State Phys.* **20** 1069
[20] Wiesenekker G, te Velde G and Baerends E J 1988 *J. Phys. C: Solid State Phys.* **21** 4263
[21] Wiesenekker G and Baerends E J 1991 *J. Phys.: Condens. Matter* **3** 6721
[22] Broido D A and Sham L J 1985 *Phys. Rev.* B **31** 888
Ando T 1985 *J. Phys. Soc. Japan* **54** 1528
Ekenberg U and Altarelli M 1985 *Phys. Rev.* B **32** 3712
[23] Janak J F 1971 *Computational Methods in Band Theory* ed P M Marcus, J F Janak and A R Williams (New York: Plenum) pp 323–39
[24] Gilat G 1973 *Phys. Rev.* B **7** 891
[25] Eschrig H 1989 *Optimized LCAO-Method (Springer Research Report in Physics)*
[26] Stormer H L, Schlesinger Z, Chang A, Tsui D C, Gossard A C and Wiegmann W 1983 *Phys. Rev. Lett.* **51** 126